

# Lidar observation of aerosol stratification in the lower troposphere over Pune during pre-monsoon season of 2006

P ERNEST RAJ\*, S K SAHA, S M SONBAWNE, S M DESHPANDE, P C S DEVARA,  
Y JAYA RAO, K K DANI and G PANDITHURAI

*Indian Institute of Tropical Meteorology, Pashan Road, Pune 411 008, India.*

*\*e-mail: ernest@tropmet.res.in*

Lidar observations of aerosol vertical distributions in the lower troposphere along with observations of horizontal and vertical winds from collocated UHF radar (Wind Profiler) over a tropical Indian station, Pune during the pre-monsoon season (March–May) of 2006 as part of an ISRO-GBP national campaign (ICARB) have been examined. Lidar vertical profiles showed high aerosol concentrations in the surface layers and a subsequent gradual decrease with height. Results showed the presence of an elevated stratified aerosol layer around 2000–3500 m height which persisted throughout the months of March and April. Observed strong vertical gradients in both horizontal and vertical winds in the lower troposphere seem to be a possible cause for the formation of elevated aerosol layers. Further, high daytime temperatures accompanied by dry conditions at the surface help to enhance the aerosol loading in the lower layers over this location.

---

## 1. Introduction

Concentration and composition of tropospheric aerosols are highly variable both temporally and spatially. Aerosols together with other atmospheric gaseous constituents modulate the intensity of incoming solar radiation as well as the outgoing long-wave radiation. Hence they can directly and indirectly influence the radiation budget of the atmosphere (WCP-55 1983; IPCC 1992; Charlson *et al* 1992). The clear-sky climate forcing by anthropogenic aerosols has been shown to be of sufficient magnitude to mask the effects of anthropogenic greenhouse gases. The cloudy-sky forcing by these aerosols, wherein aerosol cloud condensation nuclei are increased, thereby increasing cloud droplet concentrations and cloud albedo and possibly influencing cloud persistence, may also be quite significant (IPCC 1992; DOE 1993). Aerosols in the troposphere currently pose the largest single uncertainty in calculating the net forcing due to anthropogenic changes in the chemical composition

of the atmosphere. It is therefore important to quantify forcing by anthropogenic aerosols and minimize uncertainties in the calculated forcings. For this purpose, more systematic observations in different environments including oceanic regions are needed. This will also require quantification of the natural aerosol. Indian Ocean Experiment (INDOEX) conducted in the recent past showed that every year from December to April anthropogenic haze spreads over most of north Indian Ocean and south and southeast Asia and it has significant contribution to regional climate forcing (e.g., Ramanathan *et al* 2001). Because of the dominant influence of anthropogenic emissions from industries, domestic heating/cooking systems and vehicular traffic, the aerosols in the urban centers have a special character. Mobilization, transportation and deposition of particulate pollutants is a concern of several disciplines like climatology, ecology and geology and there is overwhelming evidence that lower tropospheric aerosols can be transported over large distances, even

**Keywords.** Lidar, wind profiler, aerosol layer, aerosol column content.

inter-continently (Hobbs *et al* 1971; Mitev *et al* 2005).

In view of the above reasons, it is crucial that a research program be established to quantify the climate forcing by anthropogenic aerosols in order to understand and be able to predict the overall meteorological and climatic consequences of large-scale, spatially non-uniform changes in the chemical composition of the atmosphere. The prime components of such an observational program should include surface-based (both land and ship) observations both for continuous and intensive periods, airborne and satellite-borne observations together with regional climate modeling. To achieve some of these objectives, ISRO-GBP has organized the Integrated Campaign for Aerosol, gases and Radiation Budget (ICARB) during the pre-monsoon months of March–May 2006. The campaign envisages well co-ordinated observations of atmospheric aerosols and gases over the Indian land region and over the marine regions surrounding the Indian subcontinent during the pre-monsoon period. Lidar observations of vertical distribution of atmospheric aerosols in the lower troposphere in conjunction with wind profiler derived data and surface meteorological parameters over Pune (18°32'N, 73°51'E, 559 m Above Mean Sea Level), India during the ICARB (March–May 2006) campaign are presented and discussed in this paper.

## 2. Equipment and data

Pune is an urban continental tropical station located on the lee side of the Western Ghat mountain range and it is about 200 km inland to the east of the Arabian Sea coast. This station is under the influence of south westerly winds during the months of June to September and during the other months especially in winter surface level winds are predominantly easterly or northeasterly. The lidar site is surrounded by small hillocks as high as 760 m AMSL.

Systematic Argon ion lidar observations of atmospheric aerosols in the nocturnal lower troposphere including time-height variations in aerosols has been in progress at the Indian Institute of Tropical Meteorology, Pune since October 1986 (Ernest Raj *et al* 1997; Devara *et al* 2002). The lidar system operated in bistatic mode essentially comprises a continuous wave Argon ion laser (Lexel Model 95-4) operated at 514.5 nm wavelength as transmitter and a 25-cm Newtonian telescope-photomultiplier assembly as the receiver. The laser beam divergence is  $0.283 \times 10^{-6}$  steradian and the field of view of the receiver is about  $0.75^\circ$  with a collecting area of  $490 \text{ cm}^2$ . The average

output power of the laser employed in the experiments is 400 mW. At the receiver-end a narrow band interference filter of 1 nm FWHM is used. Detailed specifications of the Argon ion lidar system are given in several earlier publications of the authors (e.g., Devara and Ernest Raj 1987; Ernest Raj and Devara 1989). The movement of the telescope (both elevation and azimuth), selection of the filter, shutter for laser beam interruption, data acquisition, etc., are all controlled by the computer remotely. The computer-controlled stepper motor arrangement enables telescope elevation increment of  $0.1^\circ$ . The transmitter and receiver are separated by a distance of about 60 m in the same horizontal plane. However this small separation distance limits the upper altitude of probing and height resolution at larger elevation angles. In the present experiment laser scattered signal strength is collected at 48 height intervals between 50 m and 8600 m above ground level. But because of the small separation distance, height interval is not uniform throughout, especially at upper altitudes. A more or less uniform height interval of 50 m could be maintained from surface to about 1500 m altitude. Above this altitude the height interval corresponds to telescope elevation angle increment of  $0.1^\circ$ . In bistatic mode of operation, the height resolution is dependent on the common scattering volume, i.e., the overlapping of the laser beam and telescope field of view. The height resolution is good up to 1000 m altitude (about  $\pm 100 \text{ m}$ ), fairly good up to 3000 m altitude (about  $\pm 450 \text{ m}$  at 2000 m,  $\pm 750 \text{ m}$  at 2500 m,  $\pm 1100 \text{ m}$  at 3000 m) but significant overlapping of adjacent common scattering volumes occurs above 5000 m. However, these height resolutions are obtained from the total vertical extent of the scattering volume from bistatic lidar geometry which roughly comprises a central cylindrical volume with conical volumes on either end. The maximum scattered intensity may be from the aerosols in the central cylindrical volume. Therefore the actual height resolutions would be almost 50% of what has been mentioned above. The scattered signal strength and subsequently the aerosol concentration in the vertical profiles are indicated at the height corresponding to the center of scattering volume. Because of the limitation in height resolution all the lidar vertical profiles in this study have been shown only up to a height of 5 km.

The laser scattered intensity profiles obtained from the experiment have been converted to aerosol number density (aerosol concentration,  $\text{cm}^{-3}$ ) profiles by employing inversion techniques (Parameswaran *et al* 1984; Devara and Ernest Raj 1987; Devara *et al* 2002; Ernest Raj *et al* 2004). The prevailing environment over the experimental site is urban and the aerosol type is assumed

to be a mixture of water-soluble and dust-like aerosols. It is also assumed in the computations that aerosols are homogeneous spherical particles characterized by a single refractive index. Further, aerosol size distribution was assumed to follow a modified power-law distribution. The Mie theory governs the scattering due to aerosol particles, whereas molecular scattering is governed by Rayleigh theory and since at any given instant, atmosphere contains both aerosols and molecules; the measured scattered signal is corrected for Rayleigh scatter to the extent possible. Some of the assumptions mentioned above are made to permit estimation of aerosol concentration from scattered signal strength. Such assumptions could introduce an element of error (about 10%) in aerosol concentration estimation. However since altitude structure and temporal evolutions are mostly investigated using such data, the error perhaps does not affect the overall results to a large extent.

A 404 MHz Wind Profiler (UHF radar) system has been in continuous operation at Pune since June 2003. The Wind Profiler is situated about 300 m away from the lidar site. It has average power aperture product of about  $2 \times 10^5 \text{ Wm}^2$ . The system consists of a dual polarized coaxial collinear antenna array, the two arrays aligned along true N-S and E-W directions. The arrays produce three beams, two tilted beams; one along the east and the other along south and the third beam looking at zenith. The profiler measures the radial velocities along these three beams by analyzing the observed Doppler shifted signals adopting the Doppler Beam Swinging technique. Such a configuration enables simultaneous measurement of all three components (zonal, meridional and vertical) of the wind field. The system has height coverage from 1.05 km to about 6–10 km (upper altitude depending on weather conditions) with a height resolution of 300 m. The detailed technical specifications of the Pune Wind Profiler System inclusive of signal processing, data quality control and preliminary validation of the wind profiler data products with the other conventional instruments have been given in a recent publication (Pant *et al* 2005). Horizontal (zonal and meridional) and vertical wind profiles obtained with this system at 1700 hrs Local Time (LT) on all the days during the three-month period, March–May 2006 are available to examine the influence of winds and wind shears on aerosol vertical distributions in the lower troposphere. All the vertical distances (altitudes) mentioned in this study, both in the case of lidar and wind profiler observations, refer to altitudes above ground level.

### 3. Results and discussion

Argon ion lidar at Pune was actually planned to be operated on every alternate day during the ICARB observational period from 1 March to 31 May, 2006. But due to unfavourable sky conditions and unforeseen technical problems, good data of aerosol vertical distributions is available only on 21 days spread out in the three-month period (i.e., 8 days in March, 7 days in April and on 6 days in May). The lidar aerosol profiles are obtained during the post sunset period (between 1900 and 2000 h LT). Figure 1(a) shows vertical profiles (in the altitude region 50–5000 m) of aerosol number density ( $\text{cm}^{-3}$ ) on two typical days of March 2006 (1 and 13). Aerosol concentrations as observed at this location for several years (Ernest Raj and Devara 1989; Devara *et al* 1995) are in general, higher at surface levels ( $\sim 4500 \text{ cm}^{-3}$ ) up to about 500 m and then gradually decrease with height. One can notice enhancement in concentration (layer formations) around 1400 m and 3000 m on 1 March and a significant layer peak around 2200 m on 13 March. Similarly vertical profiles of aerosol number density on two typical days of April 2006 (3 and 5) are shown in figure 1(b). Here again broad layer formations in the 2000 to 3800 m altitude range can be seen on both the days. Such elevated layers were not evident in the individual profiles obtained in the last week of April and during May 2006. The monthly mean aerosol concentration profiles for March, April and May are shown in figure 2(a) along with the standard deviations at the respective heights (as horizontal bars). For comparison, corresponding monthly mean profiles obtained from the lidar data collected during the period 1987–1994 have also been included in the figure (as dashed lines). Elevated layer formation can be seen in the mean profiles also, especially during April. Aerosol concentrations above 1000 m altitude during March 2006 and above 2000 m during April 2006 are significantly higher than that observed in the corresponding long-term monthly means. On the other hand, during May 2006 the concentrations are lower, especially below 3000 m, than that obtained in the long-term mean. The variability seems to be higher during March and April, evident from the standard deviations. The overall mean vertical distribution of aerosol concentration for this three-month period is obtained (mean vertical profile of aerosol number density) and shown plotted for the altitude region 50–5000 m in figure 2(b). The thick solid line in the figure shows the 3-point running average and the horizontal bars denote standard deviations at respective heights. The shape of the vertical profile is very typical of this urban tropical location.

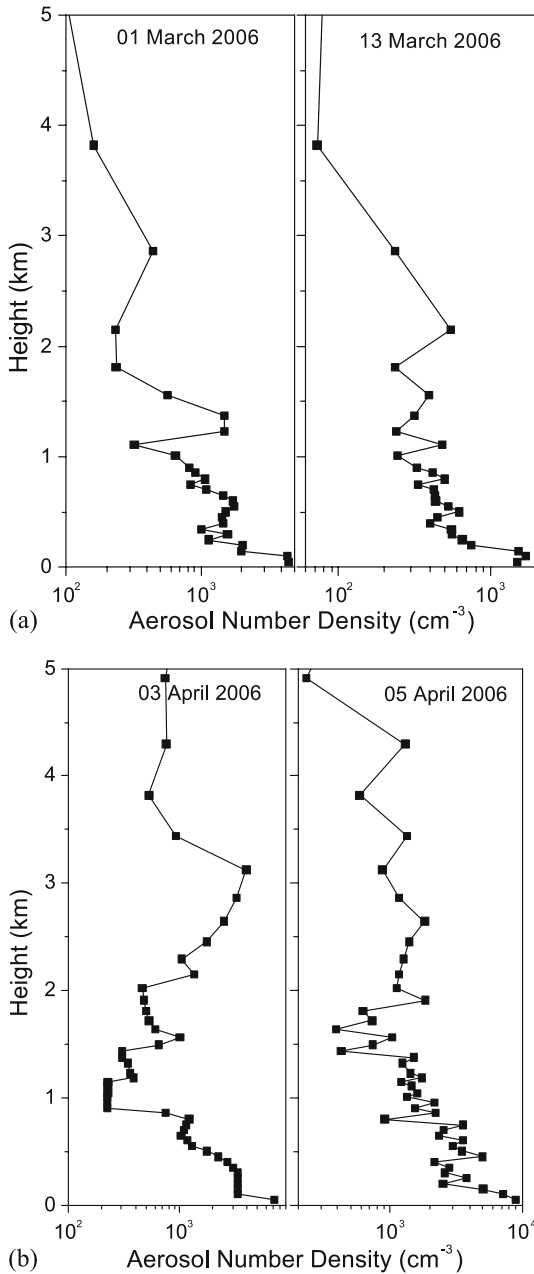


Figure 1. Lidar-derived vertical profiles of aerosol number density on two typical days (a) 1 and 13 in March 2006, and (b) 3 and 5 in April 2006.

The mean profile clearly shows high concentrations at lower heights (as high as 5000 particles/cm<sup>3</sup>), a smooth decrease with height with a smooth gradient. Occasional change/decrease observed in concentration gradient up to 1500 m is indicative of weak aerosol layers. As mentioned above, the interesting aspect of the observations during the pre-monsoon months of 2006 is the presence of a significant aerosol layer/stratification in the 1800–3000 m height region, where enhanced aerosol concentrations are observed. The lidar observations reported here were collected during clear sky

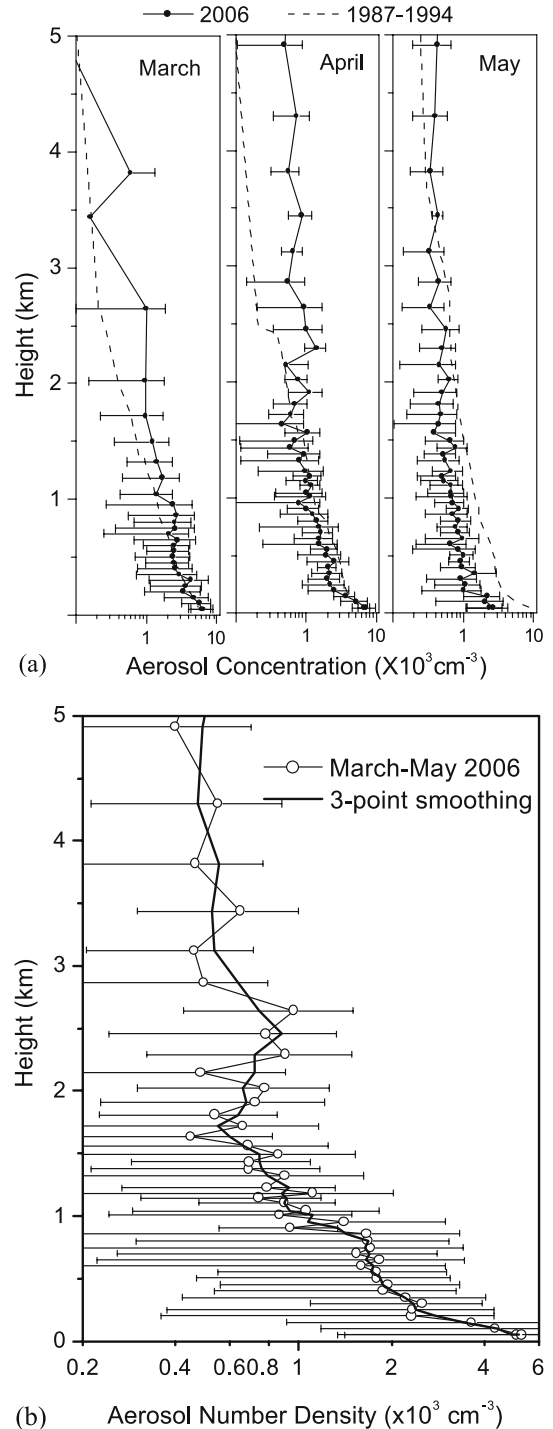


Figure 2. (a) Monthly mean vertical distribution of aerosol number density for March, April and May 2006 along with corresponding month's mean for the period 1987–1994 (horizontal bars at each height indicate standard deviation). (b) Mean vertical distribution of aerosol number density for the period 1 March–22 May 2006 (horizontal bars at each height indicate standard deviation and thick solid line indicates 3-point smoothing).

conditions. To examine the time evolution of this aerosol stratification in the lower troposphere, contour plot (time-height variation) of aerosol number

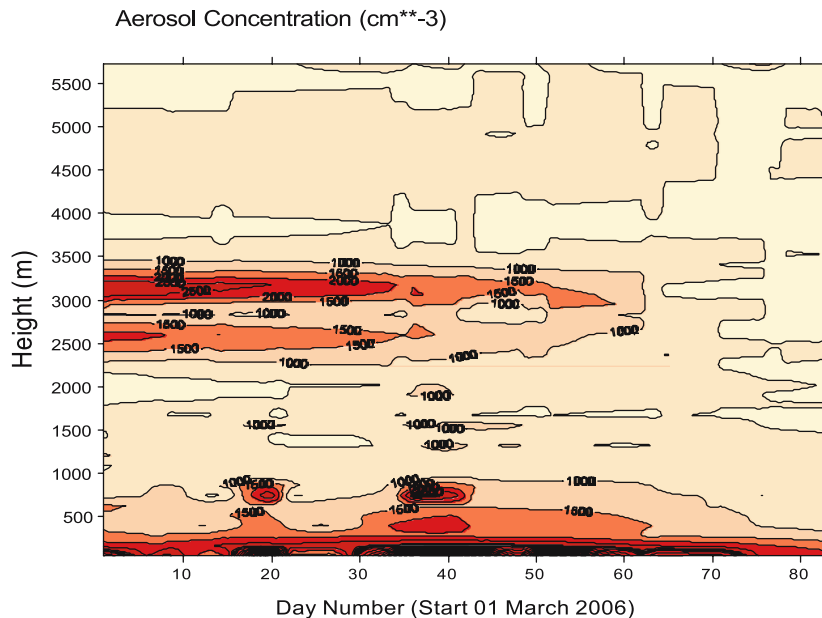


Figure 3. Time–height variation of aerosol number density in the lower troposphere during the period 1 March–22 May 2006.

density is obtained using all the available individual lidar vertical profiles up to 5500 m altitude and shown for the three-month period in figure 3. Here one can see that there indeed exists a stratified aerosol layer (of enhanced aerosol concentration) in the altitude region 2000–3500 m. This layer seems to be relatively stronger in the month of March and during the first half of April. It is however present only till the end of the month of April and is not present in May. In the second half of May clouds started appearing over the station and hence the lack of aerosol profile data during last week of the month. Occurrence of such aerosol layers/aerosol stratification in the lower troposphere has been reported in literature and various causes have been put forth. Searchlight probing of an urban atmosphere in Ontario, Canada detected various stratified aerosol layers which assumed a variety of dimensions and movements within the lower troposphere (Gschwandtner and Pengelly 1978). Lidar studies of elevated aerosol stratification extending up to 4500–5000 m above sea level over the Rhine Valley (Switzerland) under strong anti-cyclone conditions have been reported by Frioud *et al* (2003). Aerosol layers have been observed by lidar during a ‘Bise’ event in Switzerland starting at altitudes just above the PBL top till 3000–3500 m above ground level (Mitev *et al* 2005). Back trajectories were reported in this study to show long-range transport and a likely origin of aerosols from the north American region. Further, lidar observations of Ansmann *et al* (2005) over a location in south coast of China showed that in most of the observed cases the top of the

haze layer reached to heights of 1500–3000 m. Observations of aerosol concentrations over the Indian Ocean region during March 2006 using three unmanned aerial vehicles have recently been reported by Ramanathan *et al* (2007). They have mentioned that above 1 km altitude, aerosol number concentration of about  $750 \text{ cm}^{-3}$  during 4–16 March increased to  $2500 \text{ cm}^{-3}$  by 19–29 March. Thus observation of elevated layers of atmospheric aerosols over different locations, both over land and over oceanic regions has become more frequent, though the causes and sources may slightly differ from location to location.

Several studies have attempted to relate the aerosol vertical distributions and aerosol layer formation in the troposphere to winds, both speed and direction. Here in this study the UHF radar/wind profiler observations made close to the lidar site have been used to examine the possible relationship. Daily profiles of horizontal (zonal and meridional) and vertical winds available at 1700 h LT, the closest possible in time to lidar observations (1900–2000 h LT), have been collected but wind data on only those days coinciding with the lidar observation days have been used for all further analysis in this study. Figure 4 shows vertical profiles (1050–7000 m) of the three-month (March–May 2006) mean total wind speed and wind direction computed from the wind profiler data of zonal and meridional winds at 1700 h LT. Standard deviations in wind speed at corresponding heights are also depicted in the figure as horizontal bars. Wind speed shows a peak in the 3000–4000 m level and again increases beyond 5000 m. At the first

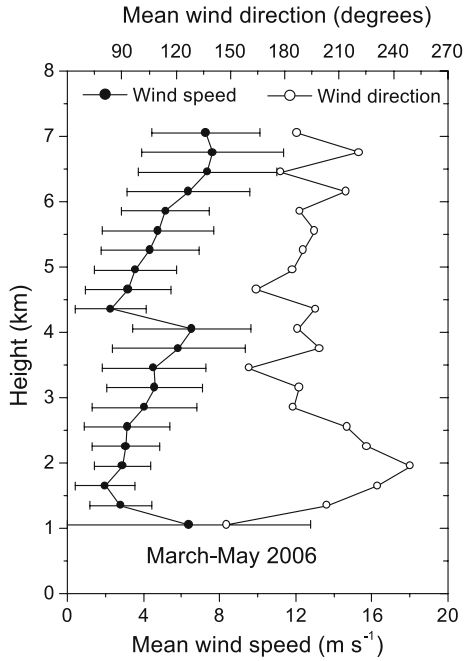
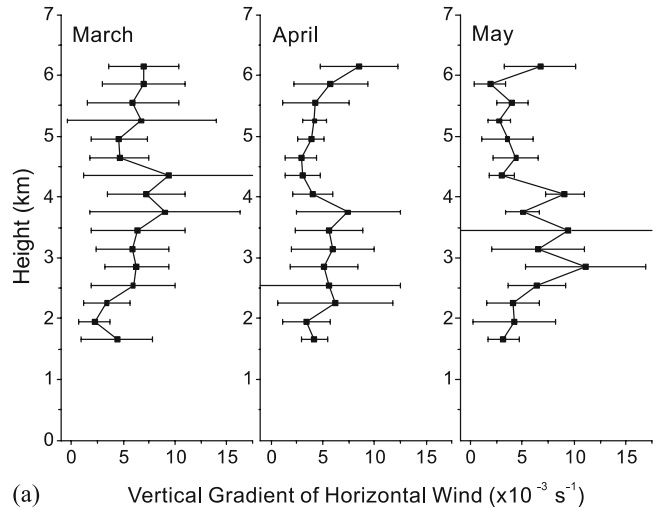


Figure 4. Height variation of mean total (horizontal) wind speed and wind direction for the period 1 March–22 May 2006 at 1700 h LT.

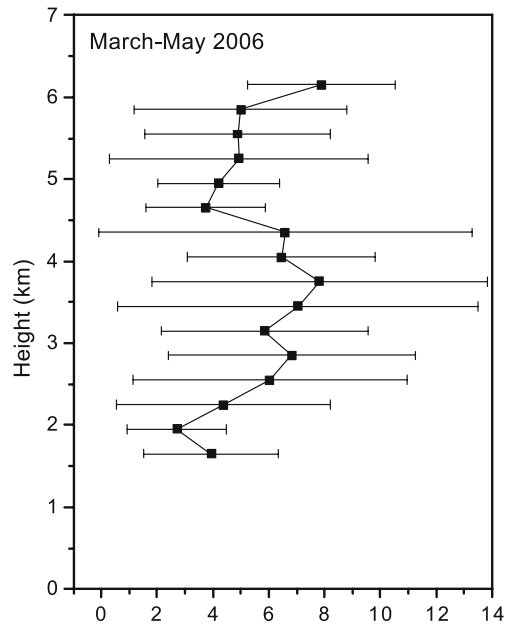
level, i.e., 1050 m, radar-derived wind information may be contaminated by ground clutter or some other reason and therefore wind speeds are sometimes unusually high or spurious at this level. For this reason the standard deviation in the three-month mean at this first level (figure 4) is also high which may not be entirely due to atmospheric reasons. The variability in horizontal wind speed (standard deviation) is relatively smaller at heights below 3000 m. Mean pre-monsoon wind at this location is predominantly south-westerly below 3000 m and it is south south-easterly in the free troposphere.

The vertical gradient of horizontal (total) wind ( $dU/dz$ ) at a particular level is estimated from the wind profiler derived zonal ( $u$ ) and meridional ( $v$ ) components as,  $dU/dz = [(du/dz)^2 + (dv/dz)^2]^{1/2}$ ; where  $dz$  is the altitude difference between two consecutive levels (300 m). The wind gradient at the  $i$ th level is taken as the mean of the gradients estimated between  $i$ th and  $(i - 1)$ th level and  $i$ th and  $(i + 1)$ th level.

Thus monthly mean vertical gradient of horizontal wind ( $dU/dz$ ) computed from the wind-profiler derived zonal and meridional wind speeds separately for the months of March, April and May is shown in figure 5(a) and the overall mean for the three months is shown in figure 5(b). The horizontal bars in both the figures indicate standard deviations at the respective heights. It can be seen that vertical gradient of horizontal wind is relatively stronger in the 2500–4500 m altitude region



(a) Vertical Gradient of Horizontal Wind ( $\times 10^{-3} \text{ s}^{-1}$ )



(b) Vertical Gradient of Horizontal Wind ( $\times 10^{-3} \text{ s}^{-1}$ )

Figure 5. (a) Height variation of monthly mean vertical gradient of horizontal wind for March, April and May 2006 at 1700 h LT. (b) Height variation of mean vertical gradient of horizontal wind for the period 1 March–22 May 2006 at 1700 h LT.

which is seen in the individual months as well as the overall three-month mean. Vertical wind velocity ( $w$ ) data again on only those days coinciding with lidar observation days has been used to compute the vertical gradient of vertical wind ( $dw/dz$ ) at a particular level  $i$ , which is also taken as the mean of the gradients estimated between the  $i$ th and  $(i - 1)$ th level and  $i$ th and  $(i + 1)$ th level as in the case of horizontal wind.

Profiles of vertical gradient of vertical wind obtained on days coinciding with the typical lidar aerosol profiles shown in figure 1(a) (1 and 13 March, 2006) and in figure 1(b) (3 and 5 April,

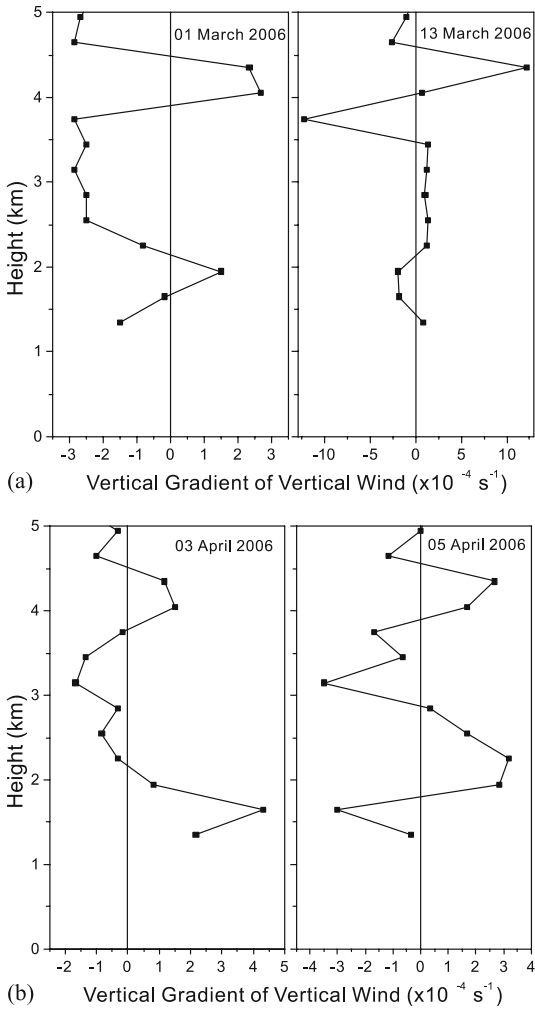


Figure 6. Height variation of vertical gradient of vertical wind on (a) 1 and 13 March 2006 at 1700 h LT and (b) 3 and 5 April 2006 at 1700 h LT.

2006) are shown plotted in figures 6(a) and 6(b) respectively. For uniformity,  $dw/dz$  profiles on the above four individual days are shown up to an altitude of 5000 m. On 1 March, a positive gradient occurs around 2000 m and becomes a strong negative gradient around 3750 m with a minimum vertical gradient around 2200 m. On this day (figure 1a) aerosol layers with peaks around 1500 m and 2800 m occurred. On the other three days also aerosol layers seem to occur around the levels where such positive  $dw/dz$  is followed by a negative  $dw/dz$  with height. It is possible that aerosols lifted up during daytime along with growth of mixed layer can get accumulated in the layer between strong vertical wind gradients. The positive and negative vertical gradients (in vertical winds) may lead to convergence and accumulation of aerosols. Profiles of monthly mean vertical gradient in vertical wind speed for the three months March, April and May 2006 along with standard deviations are

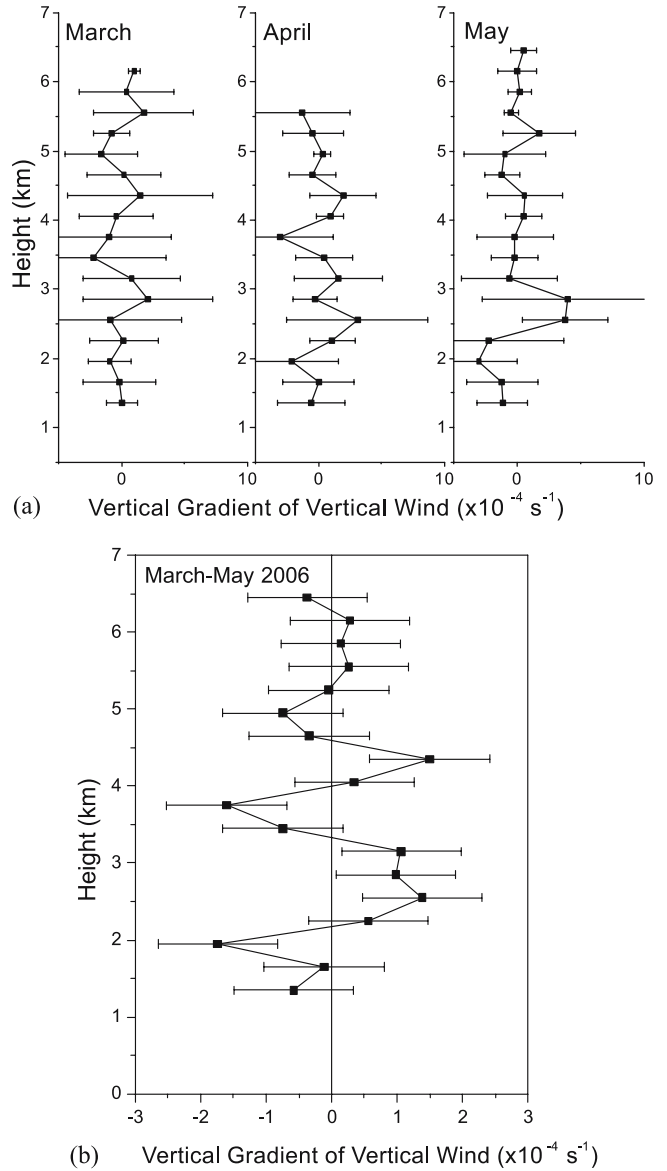


Figure 7. (a) Height variation of monthly mean vertical gradient of vertical wind for March, April and May 2006 at 1700 h LT. (b) Height variation of mean vertical gradient of vertical wind for the period 1 March–22 May 2006 at 1700 h LT.

shown in figure 7(a). Strong vertical gradients (both positive and negative) are seen in the height region 2500–4500 m. Figure 7(b) shows the overall three-month mean profile of  $dw/dz$ . It is seen that a strong positive vertical wind gradient exists around 2500 m and again a strong negative gradient around 3500 m with almost a zero gradient in between. Simultaneous observations of lidar aerosol vertical profiles thus indicated the presence of an elevated layer around the same region. Saha and Krishna Moorthy (2005) have reported the possible influence of vertical winds on aerosol loading. They also mentioned that strong convection over continental landmass favour increased vertical transport

of aerosols which are then carried by prevailing winds and deposited at locations where there is a downdraft or descent of air mass, thus providing an additional source of aerosols at locations far away from the source regions. There are reports of such long-range transport of continental aerosols from the Arabian Desert and north-west India (Jha and Krishnamurti 1998; Rajeev *et al* 2000). Thus simultaneous observations of vertical profiles of aerosols and winds reveal possible relationships especially in the formation of elevated aerosol layers which persisted for several days. The thermal structure of the lower atmosphere could also influence the vertical distribution of atmospheric aerosols, but such data are not currently available for investigations.

The role of orographic and local (surface) meteorological factors in influencing the aerosol loading over a location however, cannot be ignored. Therefore to examine how the aerosol loading (integrated aerosol concentration) in the layers close to the surface over Pune varied during this three-month campaign period and how it is related to the surface meteorological conditions, daily maximum temperature and relative humidity data from India Meteorological Department, Pune has been collected for the three-month period of ICARB campaign. Aerosol column content ( $\text{cm}^{-2}$ ) representative of the aerosol loading has been computed by integrating the individual aerosol profile on each day between the two altitude regions, 50 to 1100 m and 50 to 200 m. The first altitude region is believed to roughly fall within the average convective boundary layer at this location and the second region (50–200 m) is strongly influenced by local terrain and surface sources of particulates. The day-to-day variation of aerosol column content in these two layers starting from 1 March 2006 is plotted in figure 8. It is observed that column content in both the layers showed a similar day-to-day variation indicating predominant surface origin of aerosols in the boundary layer during the pre-monsoon season. Also percentage column content in the 50–200 m layer to the total content in the 50–1100 m layer was 20–30% in March, > 40% in April and 30–40% in May which indicates that the bulk of the aerosol load ( $\sim 40\%$ ) is confined to surface layers during this season. Day-to-day variations in aerosol column content showed that they were high for about a week in the beginning of the campaign (i.e., first week of March) and then decreased. By the end of March (day number 30 in figure 8), the column content started increasing substantially and was maximum during the first half of the month of April (up to about day number 45). During the later part of the period also it remained slightly on the higher side. Figure 9 shows simultaneous day-to-day variation of surface

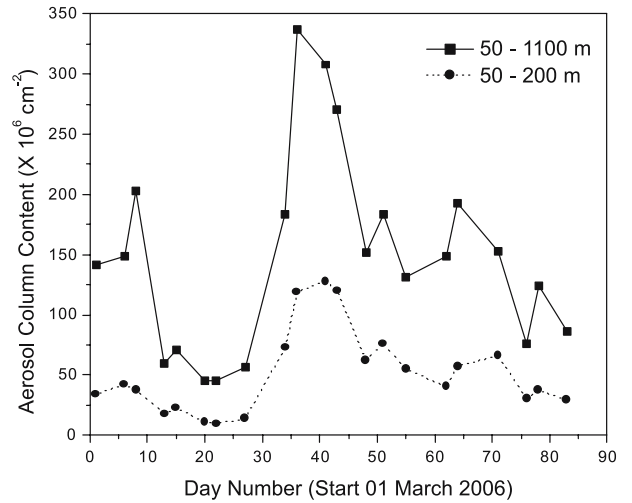


Figure 8. Day-to-day variation of lidar-derived aerosol column content in the 50–200 m and 50–1100 m levels during the period 1 March–22 May 2006.

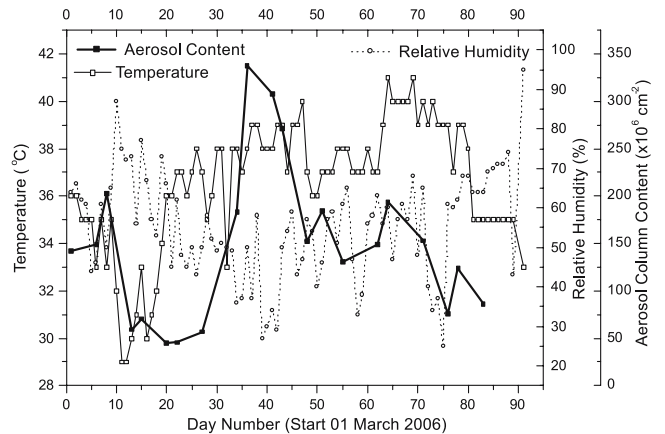


Figure 9. Day-to-day variation of aerosol column content in the 50–1100 m level, surface maximum temperature and relative humidity for the period 1 March–31 May 2006.

maximum temperature ( $^{\circ}\text{C}$ ), relative humidity (%) and lidar-derived aerosol column content in the 50–1100 m layer. Daytime surface maximum temperature was around  $36^{\circ}\text{C}$  on 1 March, decreased to  $30\text{--}32^{\circ}\text{C}$  during 10–20 March. It then started increasing substantially and was  $36^{\circ}\text{C}\text{--}40^{\circ}\text{C}$  after 20 March. Temperatures were as high as  $41^{\circ}\text{C}$  on a few days in May. Surface relative humidity was higher (60–80%) during March, lowest around 10 April ( $\sim 30\%$ ), and again started increasing till the end of May. Aerosol column content was observed to be substantially high when surface temperatures were high and humidity was less. On a day-to-day basis though the dataset of simultaneous observations is small, a positive correlation was obtained between aerosol column content and surface temperature with a small correlation coefficient (+0.353). Whereas, aerosol column content

and surface relative humidity showed significant negative correlation (correlation coefficient being  $-0.653$ ). Thus hot and dry daytime conditions favoured increase of particulate loading in the lower layers of the atmosphere which tend to remain as a residual layer in the late evening hours. Aerosols of surface and soil origin lifted into the lower atmosphere during daytime due to surface meteorological conditions, tend to remain as nocturnal stratified aerosol layers under conditions of strong wind shears (wind gradients) and by action of vertical motions (updrafts and downdrafts) in the lower troposphere.

#### 4. Conclusions

Vertical distributions of lower tropospheric aerosols obtained from lidar measurements at a tropical urban Indian station, Pune during the pre-monsoon (March–May 2006) national observational campaign (ICARB) showed the presence of an elevated stratified aerosol layer at around 2000–3500 m. This layer seems to have persisted continuously during the months of March and April. Strong local wind shears (vertical gradients in both horizontal and vertical winds) in the lower troposphere as observed from collocated UHF radar/wind profiler measurements seem to be aiding the formation of such elevated aerosol layers over the region. Aerosol column content (indicative of aerosol loading) in the 50–1100 m and 50–200 m layers over the location showed enhancement during the month of April. Surface layers contribute significantly to the overall loading in the boundary layer. Surface meteorological observations show that high daytime temperatures accompanied by dry atmospheric conditions (low relative humidity) can lead to increase in aerosol loading in the lower atmosphere.

#### Acknowledgements

Authors are grateful to the Director, IITM for his constant encouragement and support. Efforts of the India Meteorological Department, Pune in operating the wind profiler system and Dr. (Mrs.) R R Joshi in organizing wind profiler data processing/archiving are thankfully acknowledged. Authors are very thankful to the two anonymous reviewers whose suggestions and comments have been very helpful in finalising the manuscript.

#### References

- Ansmann A, Engelmann R, Althausen D, Wandinger U, Hu M, Zhang Y and He Q 2005 High aerosol load over the Pearl River Delta, China observed with Raman lidar and sun photometer; *Geophys. Res. Lett.* **32** doi:10.1029/2005GL023094, L13815.
- Charlson R J, Schwartz S E, Hales J M, Cess R D, Coakley J A Jr., Hansen J E and Hofmann D J 1992 Climate forcing by anthropogenic aerosols; *Science* **255** 423–430.
- Devara P C S and Ernest Raj P 1987 A bistatic lidar for aerosol studies; *IETE Tech. Rev.* **4** 412–415.
- Devara P C S, Ernest Raj P, Sharma S and Pandithurai G 1995 Real-time monitoring of atmospheric aerosols using a computer-controlled lidar; *Atmos. Environ.* **29** 2205–2215.
- Devara P C S, Maheskumar R S, Ernest Raj P, Pandithurai G and Dani K K 2002 Recent trends in aerosol climatology and air pollution as inferred from multi-year lidar observations over a tropical urban station; *Int. J. Climatol.* **22** 435–449.
- DOE (Department of Energy) 1993 Quantifying and minimizing uncertainty of climate forcing by anthropogenic aerosols; DOE/NBB-0092T, Contract No. W-7405-Eng-48, pp. 53.
- Ernest Raj P and Devara P C S 1989 Some results of lidar aerosol measurements and their relationship with meteorological parameters; *Atmos. Environ.* **23** 831–838.
- Ernest Raj P, Devara P C S, Maheskumar R S, Pandithurai G and Dani K K 1997 Lidar measurements of aerosol column content in an urban nocturnal boundary layer; *Atmos. Res.* **45** 201–216.
- Ernest Raj P, Devara P C S, Pandithurai G, Maheskumar R S and Dani K K 2004 Some atmospheric aerosol characteristics as determined from laser angular scattering measurements at a continental urban station; *Atmosfera* **17** 39–52.
- Frioud M, Mitev V, Matthey R, Habreli C H, Richner H, Werner R and Vogt S 2003 Elevated aerosol stratification above the Rhine Valley under strong anticyclonic conditions; *Atmos. Environ.* **37** 1785–1797.
- Gschwandtner G and Pengelly L D 1978 Measurement of the frequency and location of stratified aerosol layers using a searchlight probing technique; *Boundary-Layer Meteorol.* **14** 361–368.
- Hobbs P V, Bluhm G and Ohtake T 1971 Transport of ice nuclei over the North Pacific Ocean; *Tellus* **23** 28–39.
- IPCC (Intergovernmental Panel on Climate Change) 1992 Climate Change 1992: Supplementary Report to the IPCC Scientific Assessment; Houghton J H, Callander B A and Varney S K (eds) WMO/UNEP (Cambridge University Press) 62–64.
- Jha B and Krishnamurti T N 1998 Real-time meteorological atlas during pre-INDOEX field phase; *Florida State University Rep.* **98(08)** 104 pp.
- Mitev V, Matthey R, Frioud M, Srivastava M K, Eckhardt S and Stohl A 2005 Backscatter lidar observation of the aerosol stratification in the lower troposphere during winter Bise: a case study; *Meteorologische Zeitschrift* **14** 663–669.
- Pant G B, Joshi R R, Damle S H, Deshpande S M, Singh N, Vashistha R D, Neekhra P, Chande J V, Kulkarni A A and Pillai J S 2005 Wind profiler and radio acoustic sounding system at IMD, Pune: some preliminary results; *Curr. Sci.* **88** 761–774.
- Parameswaran K, Rose K O and Krishna Murthy B V 1984 Aerosol characteristics from bistatic lidar observations; *J. Geophys. Res.* **89** 2541–22552.
- Rajeev K, Ramanathan V and Meywerk J 2000 Regional aerosol distribution and its long range transport over the Indian Ocean; *J. Geophys. Res.* **105** 2029–2043.

- Ramanathan V and Coauthors 2001 Indian Ocean Experiment: An integrated analysis of the climate forcing and effects of the great Indo-Asian haze; *J. Geophys. Res.* **106** 28,371–28,398.
- Ramanathan V, Ramana M V, Roberts G, Kim D, Corrigan C, Chung C and Winker D 2007 Warming trends in Asia amplified by brown cloud solar absorption; *Nature* **448** doi:10.1038/nature06019.
- Saha A and Krishna Moorthy K 2005 Interannual variations of aerosol optical depth over coastal India: relation to synoptic meteorology; *J. Appl. Meteorol.* **44** 1066–1077.
- WCP-55 (World Climate Programme) 1983 Report of the Experts Meeting on Aerosols and their Climatic Effects; Deepak A and Gerber H E (eds) WCRP, ICSU/WMO, pp. 107.

*MS received 23 July 2007; revised 24 October 2007; accepted 25 October 2007*